

University of Groningen

**Accurate description of charge transport in organic field effect transistors using an experimentally extracted density of states**

Roelofs, W. S. C.; Mathijssen, S. G. J.; Janssen, R. A. J.; de Leeuw, D. M.; Kemerink, M.

*Published in:*

Physical Review. B: Condensed Matter and Materials Physics

*DOI:*

[10.1103/PhysRevB.85.085202](https://doi.org/10.1103/PhysRevB.85.085202)

**IMPORTANT NOTE: You are advised to consult the publisher's version (publisher's PDF) if you wish to cite from it. Please check the document version below.**

*Document Version*

Publisher's PDF, also known as Version of record

*Publication date:*

2012

[Link to publication in University of Groningen/UMCG research database](#)

*Citation for published version (APA):*

Roelofs, W. S. C., Mathijssen, S. G. J., Janssen, R. A. J., de Leeuw, D. M., & Kemerink, M. (2012). Accurate description of charge transport in organic field effect transistors using an experimentally extracted density of states. *Physical Review. B: Condensed Matter and Materials Physics*, 85(8), 085202-1-085202-6. [085202]. <https://doi.org/10.1103/PhysRevB.85.085202>

**Copyright**

Other than for strictly personal use, it is not permitted to download or to forward/distribute the text or part of it without the consent of the author(s) and/or copyright holder(s), unless the work is under an open content license (like Creative Commons).

The publication may also be distributed here under the terms of Article 25fa of the Dutch Copyright Act, indicated by the "Taverne" license. More information can be found on the University of Groningen website: <https://www.rug.nl/library/open-access/self-archiving-pure/taverne-amendment>.

**Take-down policy**

If you believe that this document breaches copyright please contact us providing details, and we will remove access to the work immediately and investigate your claim.

Downloaded from the University of Groningen/UMCG research database (Pure): <http://www.rug.nl/research/portal>. For technical reasons the number of authors shown on this cover page is limited to 10 maximum.



# Accurate description of charge transport in organic field effect transistors using an experimentally extracted density of states

W. S. C. Roelofs,<sup>1,2,\*</sup> S. G. J. Mathijssen,<sup>2</sup> R. A. J. Janssen,<sup>1</sup> D. M. de Leeuw,<sup>2,3</sup> and M. Kemerink<sup>1</sup>

<sup>1</sup>*Eindhoven University of Technology, P.O. Box 513, NL-5600 MB Eindhoven, The Netherlands*

<sup>2</sup>*Philips Research Laboratories, High Tech Campus 4, NL-5656 AE Eindhoven, The Netherlands*

<sup>3</sup>*University of Groningen, Nijenborgh 4, NL-9747 AG Groningen, The Netherlands*

(Received 18 December 2011; published 7 February 2012)

The width and shape of the density of states (DOS) are key parameters to describe the charge transport of organic semiconductors. Here we extract the DOS using scanning Kelvin probe microscopy on a self-assembled monolayer field effect transistor (SAMFET). The semiconductor is only a single monolayer which has allowed extraction of the DOS over a wide energy range, pushing the methodology to its fundamental limit. The measured DOS consists of an exponential distribution of deep states with additional localized states on top. The charge transport has been calculated in a generic variable range-hopping model that allows any DOS as input. We show that with the experimentally extracted DOS an excellent agreement between measured and calculated transfer curves is obtained. This shows that detailed knowledge of the density of states is a prerequisite to consistently describe the transfer characteristics of organic field effect transistors.

DOI: [10.1103/PhysRevB.85.085202](https://doi.org/10.1103/PhysRevB.85.085202)

PACS number(s): 72.80.Le, 68.37.Ps

## I. INTRODUCTION

Organic semiconductors are applied in organic photovoltaic cells, organic light emitting diodes, and organic field effect transistors (OFETs). The charge transport in organic semiconductors can be described by taking into account the disordered microstructure.<sup>1-4</sup> Crucial in the reported models is the characteristic width and shape of the density of states (DOS).<sup>5</sup> Presently, a certain shape, typically a single exponential or Gaussian, is assumed and its width and height are fitted to describe the transfer curve of field effect transistors. Several techniques have been used to extract the DOS independently from the electrical I-V characteristics.<sup>6-11</sup> A complication arises when the technique used affects the DOS itself, such as electrochemical oxidation and reduction.<sup>12</sup> Preferably a method is used that determines the DOS without changing the state of the semiconductor and without making physical contact. Here we use scanning Kelvin probe microscopy (SKPM) on functional field effect transistors as introduced by Tal *et al.*<sup>11</sup> By probing the local surface potential in the channel as a function of the applied gate bias the DOS of the organic semiconductor can be extracted. It has been shown that the use of a thick semiconducting film limits the energy range over which the DOS can be accurately determined.<sup>8</sup> Hence, we here use a monolayer of semiconducting molecules self-assembled in a field effect transistor (SAMFET).<sup>13</sup>

To model the electrical transport in a transistor, usually a shape of the DOS is assumed. By fitting the I-V characteristics, key parameters of the DOS as characteristic temperature or width are obtained. A direct validation of these parameters does not exist. Here we calculate the charge transport using a generic variable range-hopping model that allows any DOS as input. With the experimentally extracted DOS as input an excellent agreement between modeled and measured transfer curves is obtained; with a single exponential DOS an unsatisfactory description is obtained. This shows that *a priori* knowledge of the DOS is a prerequisite to accurately predict the charge transport in organic semiconductors.

## II. SKPM METHOD

The operation mechanism of SKPM is elucidated in Fig. 1. In black the figure depicts the situation where the gate is at the flat band voltage and the self-assembled monolayer (SAM) is grounded. No electrostatic field is present between the gate and the SAM and, therefore, no charges are accumulated. With SKPM a bias  $V_{\text{skpm}}$  is applied to the tip such that the electrostatic field between tip and surface is nullified. In orange the figure depicts the situation where a negative gate bias is applied to accumulate holes. The added charges fill the highest occupied molecular orbital (HOMO) of the semiconductor. Consequently the HOMO-level  $E_{\text{HOMO}}$  shifts with respect to the Fermi level  $E_F$  that is fixed by the grounded source and drain electrodes. The change of the HOMO level with respect to the Fermi level is measured with SKPM as  $\Delta E_{\text{HOMO}} = q \Delta V_{\text{skpm}}$ , with  $q$  the elementary charge.

The DOS is extracted from the measured surface potentials as function of gate bias,  $V_g$ . By decreasing the gate bias with  $\Delta V_g$ , a number of holes  $\Delta p$  is accumulated in the semiconductor:

$$\Delta p = C(\Delta V_g - \Delta V_{\text{skpm}})/q d_{\text{org}}, \quad (1)$$

in which  $C$  is the areal capacitance of the gate dielectric and  $d_{\text{org}}$  is the thickness of the semiconductor. At the same time the shift of the HOMO level  $\Delta E_{\text{HOMO}}$  is measured by SKPM. With this information the DOS of the HOMO at the Fermi level is extracted as

$$g(E_f) = \frac{\Delta p}{\Delta E_{\text{HOMO}}} = \left[ \left( \frac{dV_{\text{skpm}}}{dV_g} \right)^{-1} - 1 \right] \frac{C}{d_{\text{org}} q^2}. \quad (2)$$

This equation only holds at  $T=0$  K and when the potential distribution in the semiconductor is homogeneous. These two assumptions are considered in more detail below.

First we investigate the implications of the assumption of  $T = 0$  K. At finite temperatures a distribution of states around  $E_F$  will be filled. As a result the shift of the HOMO level will not only depend on the DOS at  $E_F$ , but also on the DOS

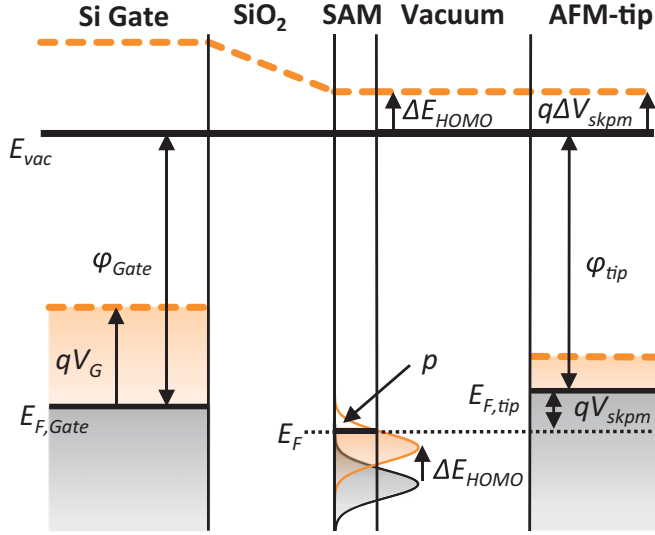


FIG. 1. (Color online) Energy band diagram of the Kelvin probe experiment. In black is depicted the situation when no gate bias is applied and with the orange dashed line the situation when a negative gate bias  $V_G$  is applied.

around  $E_F$ . This leads to a broadening of the measured DOS. For the specific case of an exponential DOS and  $T < T_0$  the hole concentration can be written as<sup>14</sup>

$$p = N_{\text{exp}} \exp\left(\frac{E_F}{k_B T_0}\right) \frac{\pi T}{T_0 \sin(\pi T/T_0)}, \quad (3)$$

in which  $T_0$  is the characteristic temperature of the exponential DOS,  $N_{\text{exp}}$  is the total number of exponential states, and  $k_B$  is Boltzmann's constant. By taking the derivative of Eq. (3) with respect to  $E_F$  and combining with Eq. (1), an equation similar to Eq. (2) is obtained, but with the right-hand side multiplied by a correction factor:<sup>14</sup>

$$g(E_f) = \left[ \left( \frac{dV_{\text{skpm}}}{dV_G} \right)^{-1} - 1 \right] \frac{C}{d_{\text{org}} q^2} \frac{T_0 \sin(\pi T/T_0)}{\pi T}. \quad (4)$$

The correction factor is close to unity as long as  $T \ll T_0$ . For temperatures around  $T_0$ , Eq. (4) no longer holds. Numerical calculations have shown that at high temperature ( $T \geq T_0$ ) it is impossible with SKPM to accurately measure the DOS; the DOS will be broadened to at least  $k_B T$ .

To circumvent calculating the numerical derivative in Eq. (4), Eqs. (1) and (3) can be combined directly into<sup>14</sup>

$$g(E_f) = \frac{C}{d_{\text{org}} q} (V_G - V_{\text{skpm}} - V_0) \frac{\sin(\pi T/T_0)}{\pi k_B T}, \quad (5)$$

where  $V_0$  is the difference between  $V_G$  and  $V_{\text{skpm}}$  when the transistor is put in the off state; all charges are depleted and  $V_0 = V_G(p=0) - V_{\text{skpm}}$ . The shape of the DOS can then directly be obtained.

If charges are nonuniformly distributed over the thickness of the semiconductor the second assumption breaks down. In conventional thin films with a thickness of more than several tens of nanometers, the assumption does not hold for any given gate bias.<sup>15</sup> Celebi *et al.* have measured the DOS for different thicknesses of the semiconductor. They indeed report an increase of the measurable range of the DOS with decreasing layer thickness.<sup>8</sup> Here we use a semiconducting monolayer. The film is only one molecule thick, which pushes the methodology to its fundamental limit.

### III. EXPERIMENT

The SAMFETs were prepared as described previously.<sup>13,16</sup> Transistor test substrates were used that consist of heavily doped silicon wafers acting as a common gate electrode, with thermally grown  $\text{SiO}_2$  as gate dielectric, and lithographically prepatterned Au source and drain electrodes. A monolayer of a functionalized quinquethiophene molecule is self-assembled from solution onto the  $\text{SiO}_2$  gate dielectric. The chemical structure is shown in the inset of Fig. 2(b). The resulting SAMFET was annealed in vacuum at 120 °C for 1 h before measuring. We used a channel width of 10 mm, channel length of 5  $\mu\text{m}$ , and a gate capacitance  $C = 17 \text{ nF/cm}^2$ . Noncontact

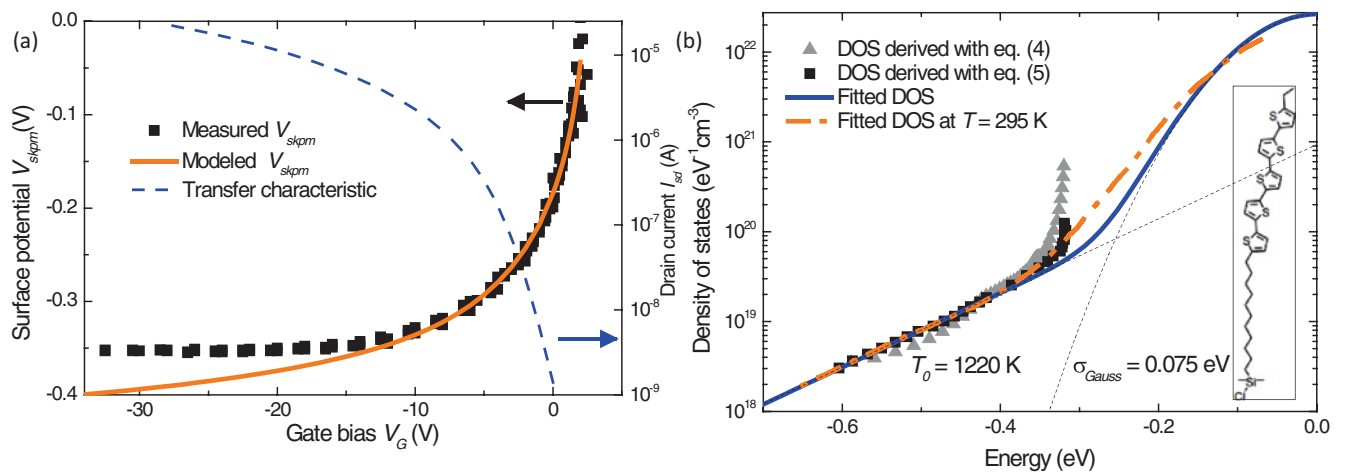


FIG. 2. (Color online) (a) Symbols: measured surface potential as function of the applied gate bias. Solid line: calculated  $V_{\text{skpm}}$  at 295 K based on the extracted DOS [solid line in (b)]. Dashed line (right axis): transfer curve at 295 K. (b) DOS vs energy. Symbols: measured values. Solid line: fitted DOS. Dash-dotted line: calculated shape of the DOS when it is measured at 295 K. The thin dashed lines are drawn to clarify the Gaussian and the exponential part of the DOS. Inset: structure of the SAM molecule.

atomic force microscopy (AFM) and SKPM measurements were performed with an Omicron VT-SPM connected to a Nanonis controller in ultrahigh vacuum ( $10^{-9}$  mbar). Pt-Ir coated AFM tips (PPP-EFM, Nanosensors,  $f_{\text{res}} \approx 70$  kHz) were used. For SKPM a 1 V AC tip voltage was applied during scanning. Before measuring the surface potential as a function of the gate voltage, a surface area of  $6 \times 3 \mu\text{m}^2$  was checked for full coverage with the SAM. *In situ* transfer characteristics were measured to check the mobility and the position of the threshold voltage of the SAMFET. During gate sweeps a low ramp speed of the gate bias ( $\sim 5$  mV/s) was used in the SKPM measurements in the subthreshold regime, in order to assure steady state and to assure that the measured surface potentials are the same for both scanning directions. Temperature-dependent transfer characteristics of the SAMFETs were measured in the linear regime (drain bias  $V_D = -2$  V) in a high-vacuum ( $10^{-6}$  mbar) probe station with a Keithley 4200.

#### IV. RESULTS AND DISCUSSION

Figure 2(a) shows the measured surface potential and the corresponding transfer curve of the SAMFET. The transistor is depleted at gate biases higher than the threshold voltage  $V_T$ . The SAM does not screen the gate, and SKPM then measures the gate voltage. When  $V_G$  is below  $V_T$  the transistor is on and the accumulated charges start to screen the gate bias. The change in  $V_{\text{skpm}}$  is then a result of the shift of the HOMO level with respect to the Fermi level and can be used to calculate the DOS as explained above. However, at gate voltages below  $-15$  V the measured surface potential becomes independent of the applied gate voltage [Fig. 2(a)]. Such invariance of the surface potential has been observed before for thicker layers, where the assumption of an independent vertical potential distribution in the semiconductor breaks down at relatively low gate fields. Here, for the SAM, the assumption breaks down at a much higher gate field and, consequently, a larger range of the DOS is probed.

The DOS as calculated from both Eqs. (4) and (5) is shown in Fig. 2(b). The deep lying states (energies below  $-0.4$  eV) that are measured in the subthreshold regime can be described by an exponential function with a width  $T_0$  of 1220 K. Comparable high  $T_0$  values are found in other direct DOS measurements on organic transistors.<sup>6–11,17</sup> However, the values are much higher than those found from direct fitting of the entire transfer characteristics with mobility models based a single exponential DOS. Typically a temperature of about 500 K is reported.<sup>4,18,19</sup> A reason for the discrepancy is a steeper DOS at higher energies.

Figure 2(b) shows that energies higher than about  $-0.4$  eV, the measured DOS indeed starts to increase and the characteristic temperature decreases. We note that the extracted points at the upper highest energies are unreliable. There the assumption of an independent potential distribution in the semiconductor breaks down. However, within the experimental accuracy the DOS increases significantly with energy.

To describe the measured DOS we add on top of the exponential DOS additional localized states. To limit the total number of states we describe this part not with an exponential function but with a Gaussian one. The DOS as extracted from

the measurements, the solid blue line in Fig. 2(b), can now be presented as

$$g(E) = \frac{N_{\text{exp}}}{k_B T_0} \exp\left(\frac{E}{k_B T_0}\right) + \frac{N_{\text{Gauss}}}{\sigma_{\text{Gauss}} \sqrt{2\pi}} \exp\left(-\frac{E^2}{2\sigma_{\text{Gauss}}^2}\right), \quad (6)$$

with  $N_{\text{Gauss}}$  the number of Gaussian states,  $\sigma_{\text{Gauss}} = 0.075$  eV the width of the Gaussian DOS,  $T_0 = 1220$  K and  $N_{\text{exp}} = 1.0 \times 10^{20} \text{ cm}^{-3}$ . The total number of states  $N_{\text{Gauss}} + N_{\text{exp}} = 5 \times 10^{21} \text{ cm}^{-3}$  is fixed by the molecule density of the SAM. The DOS is measured at finite temperatures and the measured DOS will consequently include thermal broadening. The measurements should therefore be compared to the extracted DOS including the thermal broadening. The thermally broadened extracted DOS is shown with the dash-dotted orange line in Fig. 2(b). We note that the width of the Gaussian DOS cannot accurately be extracted from the measurement. However, we show below that the functional dependence and the choice of the parameters of the additional part of the DOS are not critical. Important is that extracted DOS can accurately be described, especially the part where the DOS deviates from an exponential dependence.

The charge transport in organic semiconductors is dominated by thermally assisted hopping of charge carriers between localized states. The magnitude of the current depends on the shape of the DOS. To model the charge transport we use a hopping transport model that allows an arbitrary density of states as input. To this end we follow the Mott-Martens-type approach, which assumes that only hops from the Fermi level to a typical transport level  $E^*$  contribute to the conductivity. The transport level is the characteristic energy to which a carrier has to hop in order to contribute to the conduction. The Mott-Martens approach was previously shown to provide a good description for VRH-hopping systems.<sup>2,20</sup> In brief, the number of states,  $B$ , that can be reached in a single hop depends on the DOS, the maximum hopping distance  $R$ , and the maximum energy difference of a hop  $\Delta E$ , and is given by

$$B = \pi R^2 d_{\text{org}} \int_{E_F}^{E_F + \Delta E} g(E - E_{\text{HOMO}}) dE. \quad (7)$$

The onset of macroscopic conduction is reached when a percolating path is formed. This occurs when each site is connected to a critical number of bonds  $B_c$ . Percolation theory has shown that for a two-dimensional hopping medium such as the present SAMFET  $B_c = 4.5$ .<sup>21</sup>

In order to calculate the integral in Eq. (7), the position of the Fermi level with respect to the HOMO level has to be known. The Fermi level depends on the charge density accumulated in the channel. This density,  $p(V_g)$ , is electrostatically induced by the gate bias and follows from Eq. (1) as  $p(V_g) = (V_g - V_{\text{skpm}} - V_0)C/qd_{\text{org}}$ . In calculating the charge density the spatial variation of the potential as a result of the applied drain bias is taken into account as described previously.<sup>18</sup> The position of the Fermi level with respect to the HOMO level can now be obtained by numerically solving

$$p(V_g) = \int f(E - E_F) g(E - E_{\text{HOMO}}) dE, \quad (8)$$



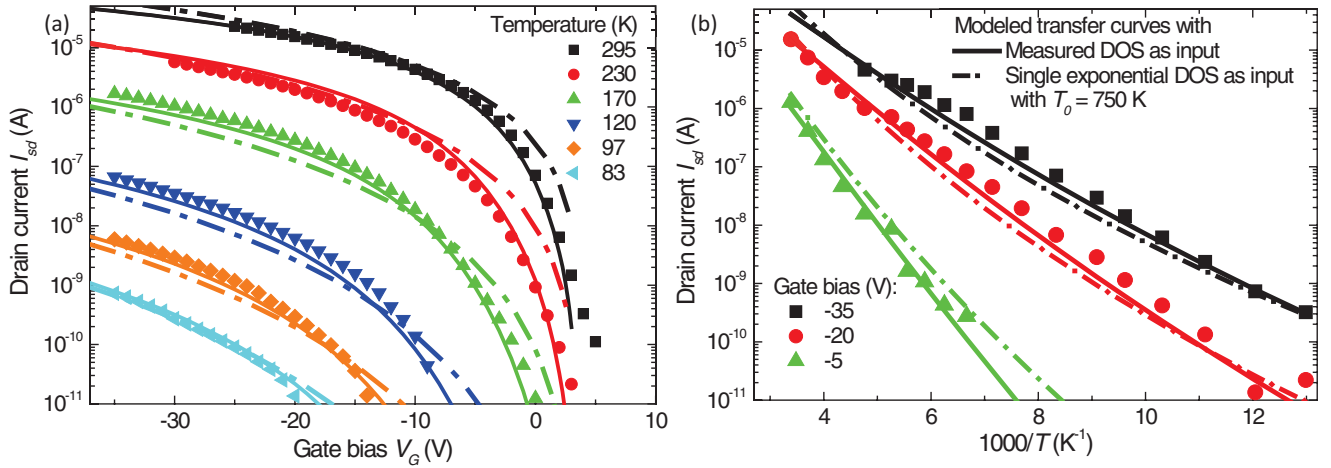


FIG. 3. (Color online) The source-drain current vs applied gate bias (a) and vs temperature (b). Symbols: measured data. The data is fitted with the numerical VRH model described in the text using the measured DOS as input (solid lines,  $\alpha^{-1} = 0.41$  nm), and using a single exponential DOS as input (dash-dotted lines,  $T_0 = 750$  K,  $\alpha^{-1} = 0.58$  nm).

where the integral runs over all energies and where  $f$  is the Fermi-Dirac distribution function.

The probability  $P$  for a charge carrier to hop over a spatial distance  $R$  with energetic distance  $\Delta E$  ( $\Delta E > 0$ ) is given by the Miller-Abrahams expression<sup>22</sup>  $P(R, \Delta E) = \exp(-2\alpha R - \Delta E/k_B T)$  where  $\alpha^{-1}$  is a measure for the localization length. The values of  $R$  and  $\Delta E$  are varied to optimize the probability  $P(R, \Delta E)$ , under the constraint that each site is connected to the critical number of bonds  $B = B_C$ . The values obtained for  $R$  and  $\Delta E$  are the typical hopping distance  $R^*$  and the typical activation energy  $\Delta E^*$ . The calculated activation energy and hopping distance are a function of gate bias and temperature. Finally, the conductivity  $\sigma$  is assumed to be proportional to this optimized value of  $P$ :  $\sigma(p, T) = \sigma_0 P(R^*, \Delta E^*)$ , where  $\sigma_0$  is a conductivity prefactor. The hopping model can be used to calculate the electrical transport in a field effect transistor. The input parameters are the shape and magnitude of the DOS,  $g(E)$ , and the localization length  $\alpha^{-1}$ .

The transfer curves of the SAMFET, source drain current as a function of gate bias, are measured for temperatures between 83 and 295 K and presented in Fig. 3(a). We first fitted the measured current using a single exponential DOS. The best fit is obtained for a characteristic temperature of 750 K and is presented by the dash-dotted lines. A good agreement is obtained in accumulation at high gate biases. In the subthreshold region, up to a gate bias of  $-10$  V, the calculated current significantly deviates from the measured current. This discrepancy is expected because SKPM measurements clearly show that in this bias range the characteristic temperature of the DOS is 1220 K, instead of 750 K. A good description of the transfer curves over the entire gate bias range is obtained using the extracted DOS. The calculated currents are presented in Fig. 3(a) by the fully drawn curves. The input parameters were a localization length of 0.48 nm, a characteristic temperature of the exponential part of the DOS as 1220 K and a width of the Gaussian part of the DOS of 0.075 eV. The excellent agreement for low gate biases follows directly from the measured exponential density of

states. At higher bias an excellent agreement is obtained due to the increase of the extracted DOS at higher energies. The calculated currents are insensitive to the width of the Gaussian DOS. Comparable currents were obtained using  $\sigma_{\text{Gauss}} = 0.09$  eV and  $\sigma_{\text{Gauss}} = 0.06$  eV.<sup>14</sup> The origin of this insensitivity as well as the origin of the nonconstant activation energy is discussed below.

The drain current as a function of temperature is presented in Fig. 3(b) for gate biases between  $-5$  and  $-35$  V. The current does not follow a simple Arrhenius behavior. The activation energy as calculated above is temperature dependent; it increases with decreasing temperature. The current is first calculated using the single exponential DOS with characteristic temperature of 750 K, similar to Fig. 3(a). The calculated currents are presented by the dash-dotted lines. A reasonable agreement is obtained. A much better agreement, however, is obtained when the current is calculated using the extracted DOS, presented by the solid lines.

The current and activation energy follow from the position of the Fermi level in the DOS and the transport level  $E^*$ . The Fermi level is calculated from the extracted DOS by Eq. (9) and presented by the fully drawn line in Fig. 4(a). The three lines correspond to temperatures between 77 and 295 K. The top  $x$  axis represents the gate bias, and the bottom  $x$  axis the corresponding induced charge density. The transport level  $E^*$  is given by the Fermi energy plus the typical activation energy  $\Delta E^*$ , derived above. The transport level is presented for temperatures between 77 and 295 K in Fig. 4(a) as the dash-dotted lines. The activation energy decreases with increasing charge density.

At low gate bias the Fermi level is located in the exponential part of the DOS. Therefore in the semilogarithmic representation a straight line is obtained. At higher bias the Fermi level is located in the Gaussian part of the extracted DOS. Slight variations in the width of the DOS therefore have a minor influence on the Fermi energy and hence on the quality of the fitted transfer curves. For this reason the DOS at those energies can be equally well be described by an exponential function. This shows that the functional dependence for the

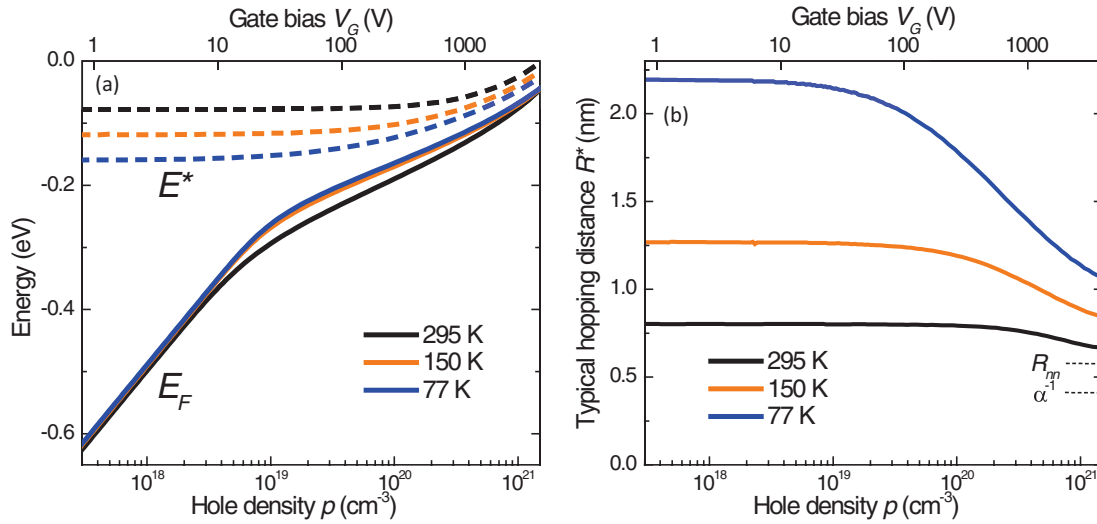


FIG. 4. (Color online) (a) Calculated position of the Fermi level  $E_F$  (solid lines) and the typical transport energy  $E^*$  (dashed lines) as function of the charge density  $p$  (bottom axis) and of the corresponding gate bias (top axis). (b) Calculated values for the typical hopping distance  $R^*$  as function of the charge density  $p$  (bottom axis) and of the corresponding gate bias (top axis). The situation for three temperatures is depicted with three different colors.

shape of the DOS is not critical for the fit of the transfer curves.

To test the internal consistency of our variable range-hopping model we have also calculated the typical hopping distance  $R^*$ . The distances are presented as a function of induced charge density and temperature in Fig. 4(b). Firstly, since the charge transport sites are assumed to be localized, the hopping distance should be larger than the localization length which is indeed the case. Secondly, we find for all conditions that the hopping distance is larger than the nearest-neighbor distance  $R_{nn}$ , calculated from the areal density of thiophene units as 0.58 nm, which is a prerequisite for true variable range hopping. The calculations show that the system approaches nearest-neighbor hopping at very high temperature and charge density.

## V. CONCLUSION

In summary, we have measured the density of states using SKPM. The DOS can be extracted when the potential distribution perpendicular to the channel is homogeneous. The thicker the semiconductor, the smaller the part of the DOS that can reliably be probed. Here we use a self-assembled

monolayer field effect transistor (SAMFET). The thickness is comparable to the thickness of the accumulation layer which has allowed us to extract the DOS over a large energy range. The DOS extracted at low energies consists of an exponential distribution of deep states with a characteristic temperature of 1220 K. The measurements show that at higher energies the DOS increases. The additional localized states are represented by a Gaussian function. To model the charge transport in the SAMFET we use a hopping transport model that allows any arbitrary density of states. With a single exponential DOS the transfer curves cannot adequately be described. However, with the experimentally extracted DOS as input a near-perfect agreement is obtained. This shows that detailed knowledge of the density of states is a prerequisite to consistently describe the transfer characteristics of organic field effect transistors.

## ACKNOWLEDGMENTS

We would like to thank F. Gholamrezaie for preparation of the SAMFETs. We gratefully acknowledge financial support from the Dutch program NanoNextNL.

\*w.s.c.roelofs@tue.nl

<sup>1</sup>G. Horowitz and P. Delannoy, *J. Appl. Phys.* **70**, 469 (1991).

<sup>2</sup>R. Coehoorn, W. F. Pasveer, P. A. Bobbert, and M. A. J. Michels, *Phys. Rev. B* **72**, 155206 (2005).

<sup>3</sup>D. Oberhoff, K. P. Pernstich, D. J. Gundlach, and B. Batlogg, *IEEE Trans. Electron Devices* **54**, 17 (2007).

<sup>4</sup>M. C. J. M. Vissenberg and M. Matters, *Phys. Rev. B* **57**, 12964 (1998).

<sup>5</sup>N. Tessler, Y. Preezant, N. Rappaport, and Y. Roichman, *Adv. Mater.* **21**, 2741 (2009).

<sup>6</sup>J. Puigdollers, A. Marsal, S. Cheylan, C. Voz, and R. Alcubilla, *Org. Electron.* **11**, 1333 (2010).

<sup>7</sup>W. L. Kalb, S. Haas, C. Krellner, T. Mathis, and B. Batlogg, *Phys. Rev. B* **81**, 155315 (2010).

<sup>8</sup>K. Celebi, P. J. Jadhav, K. M. Milaninia, M. Bora, and M. A. Baldo, *Appl. Phys. Lett.* **93**, 083308 (2008).

<sup>9</sup>S. Yogeve, E. Halpern, R. Matsubara, M. Nakamura, and Y. Rosenwaks, *Phys. Rev. B* **84**, 165124 (2011).

<sup>10</sup>W. Y. So, D. V. Lang, V. Y. Butko, X. L. Chi, J. C. Lashley, and A. P. Ramirez, *J. Appl. Phys.* **104**, 054512 (2008).

- <sup>11</sup>O. Tal, Y. Rosenwaks, Y. Preezant, N. Tessler, C. K. Chan, and A. Kahn, *Phys. Rev. Lett.* **95**, 256405 (2005).
- <sup>12</sup>I. N. Hulea, H. B. Brom, A. J. Houtepen, D. van Maekelbergh, J. J. Kelly, and E. A. Meulenkaamp, *Phys. Rev. Lett.* **93**, 166601 (2004).
- <sup>13</sup>S. G. J. Mathijssen, E. C. P. Smits, P. A. van Hal, H. J. Wondergem, S. A. Ponomarenko, A. Moser, R. Resel, P. A. Bobbert, M. Kemerink, R. A. J. Janssen, and D. M. de Leeuw, *Nat. Nanotechnol.* **4**, 674 (2009).
- <sup>14</sup>See Supplemental Material at <http://link.aps.org/supplemental/10.1103/PhysRevB.85.085202> for a derivation of Eqs. (3), (4) and (5) and for the modeled currents using different values of  $\sigma_{\text{Gauss}}$ .
- <sup>15</sup>I. Lange, J. C. Blakesley, J. Frisch, A. Vollmer, N. Koch, and D. Neher, *Phys. Rev. Lett.* **106**, 216402 (2011).
- <sup>16</sup>E. C. P. Smits, S. G. J. Mathijssen, P. A. van Hal, S. Setayesh, T. C. T. Geuns, K. A. H. A. Mutsaers, E. Cantatore, H. J. Wondergem, O. Werzer, R. Resel, M. Kemerink, S. Kirchmeyer, A. M. Muzafarov, S. A. Ponomarenko, B. de Boer, P. W. M. Blom, and D. M. de Leeuw, *Nature* **455**, 956 (2008).
- <sup>17</sup>D. V. Lang, X. Chi, T. Siegrist, A. M. Sargent, and A. P. Ramirez, *Phys. Rev. Lett.* **93**, 086802 (2004).
- <sup>18</sup>M. Kemerink, T. Hallam, M. J. Lee, N. Zhao, M. Caironi, and H. Sirringhaus, *Phys. Rev. B* **80**, 115325 (2009).
- <sup>19</sup>C. Tanase, E. J. Meijer, P. W. M. Blom, and D. M. de Leeuw, *Phys. Rev. Lett.* **91**, 21660 (2003).
- <sup>20</sup>H. C. F. Martens, I. N. Hulea, I. Romijn, H. B. Brom, W. F. Pasveer, and M. A. J. Michels, *Phys. Rev. B* **67**, 121203 (2003).
- <sup>21</sup>A. L. Efros and B. I. Shklovskii, *Electronic Properties of Doped Semiconductors* (Springer-Verlag, Berlin, 1984).
- <sup>22</sup>A. Miller and E. Abrahams, *Phys. Rev.* **120**, 745 (1960).